Hydrophobicity of the Pentafluorosulfanyl Group in Side Chains of Polymethacrylates by Evaluation with Surface Free Energy and Neutron Reflectivity

Xie, Yijun ; Iwata, Jun ; Matsumoto, Takuya ; Yamada, Norifumi L. ; Nemoto, Fumiya ; Seto, Hideki ; Nishino, Takashi

(Citation)
Langmuir,38(20):6472-6480

(Issue Date)
2022-05-24

(Resource Type)
journal article

(Version)
Accepted Manuscript

Hydrophobicity of Pentafluorosulfanyl Group in Side Chains of Polymethacrylates by Evaluation with Surface Free Energy and Neutron Reflectivity

Yijun Xie[a], Jun Iwata[a], Takuya Matsumoto[a], Norifumi L. Yamada[b], Fumiya Nemoto[b,c], Hideki Seto[b], and Takashi Nishino[a]**

[a] Department of Chemical Science and Engineering, Graduate School of Engineering, Kobe University, Rokko, Nada, Kobe, 657-8501, Japan

[b] Institute of Materials Structure Science, High Energy Accelerator Research Organization, 203-1 Shirakata, Tokai, Ibaraki 319-1106, Japan

[c] Department of Materials Science and Engineering, National Defense Academy, 1-10-20 Hashirimizu, Yokosuka, Kanagawa 239-8686, Japan

Key Word

Pentafluorosulfanyl group, Surface free energy, Neutron reflectivity, Hydrophobicity, Polymethacrylates

ABSTRACT

A hydrophobic surface or coating is required for surface protection, anti-fouling, adhesion, and other applications. For the achievements of the hydrophobic properties, fluorine-based coatings, such as the introduction of trifluoromethyl or difluoromethylene groups, are conventionally employed. The recent developments in synthetic chemistry have indicated other organic fluoroalkyl groups that are suitable for achieving a more hydrophobic surface. In this study, we focused on the hydrophobic properties of the pentafluorosulfanyl ($-SF_5$) group. We synthesized polymethacrylates with $-SF_5$ groups or other functional groups ($-CF_3$, $-CH_3$ and $-H$) in their side chains and evaluated their hydrophobicity based on contact angles of water and ethylene glycol, and the affinities of their films to water through neutron reflectivity measurements to demonstrate the superior hydrophobic properties of the $-SF_5$ group. The water contact angle on the polymethacrylate film with $-SF_5$ groups was larger, which suggested that the surface free energy was lower than those of the other polymethacrylate thin films with pendant side chains of $-CF_3$, $-CH_3$, and $-H$. In addition, the fitting analyses of the neutron reflectivity profiles of the thin polymer films in contact with air and water revealed the lowest affinity between water and the surface of polymethacrylate films with $-SF_5$ groups among the films of the synthesized polymers. Thus, we demonstrated the potential of pentafluorosulfanyl groups as advanced hydrophobic groups.

Introduction

A hydrophobic surface is a surface with low surface free energy that highly desired for many applications such as anti-fouling surfaces,[1–3] self-cleaning materials,[4–6] medical materials[7,8] and anti-icing surfaces.[9–11] Fluorine coating one of the most typical methods to fabricate a hydrophobic surface, and is widely accepted in wide fields of industrial production and household items in our daily life.[12,13] Fluorine coating mitigate the performance deterioration of products and increase their lifetime.[14–19] It is well known that fluorine has the highest electronegativity of all the elements and a very small atomic radius. Therefore, fluorine can form a stable covalent bond with other atoms, and fluorine-containing compounds not only exhibit hydro-/oleo-phobicity but also other excellent properties, such as resistance organic solvents, weather resistance, and lubricity, while maintaining their bulk properties.

Zisman *et al.* reported that the surface free energy is highly affected by the type of chemical species and concentrations of functional groups, and decreases in the order of $-CH_2- > -CH_3 > -CF_2- > -CF_2H > -CF_3$. This order indicates that well-aligned trifluoromethyl ($-CF_3$) groups should exhibit the "lowest" surface free energy on a solid material. In fact, the critical surface tension of $-CF_3$ has been reported to be ~6 mJ/m^2 based on extrapolation.[20,21] In a previous study, a vapor-deposited *n*-perfluoroeicosane ($C_{20}F_{42}$) film was fabricated, and its surface was composed of completely aligned $-CF_3$ groups with a highly dense hexagonal packing. The surface free energy of this film was measured to be 6.7 mJ/m^2, which is almost equal to the reported critical surface free energy of the $-CF_3$ group. Therefore, this surface was deemed to show the "lowest" surface free energy among the solid surfaces fabricated using general organic substituents.[22] However, recent developments in synthetic chemistry[23] have provided tools for preparing various advanced functional groups with lower surface energies than that of $-CF_3$.

It has been reported that pentafluorosulfanyl (−SF_5) group,[24–26] with more fluorine atoms in its chemical structure than −CF_3, has higher electronegativity[27] and significantly higher lipophilicity (Hansch hydrophobicity constant, π is 1.51 for SF_5 and 1.09 for CF_3).[28] In previous studies, aromatic compounds containing a −SF_5 substituent were reported to be less water soluble, and thus more hydrophobic than the corresponding −CF_3 derivatives.[29] Moreover, a self-assembled monolayer of SF_5-perfluoroalkyl thiol on gold surface fabricated by Gard *et al.*[30] had a water contact angle of 112°. In addition, Gard *et al.* also reported that a cast film of a polymer with –$(CF_2)_n$–SF_5 groups in its side chains exhibited a water contact angle of 112° as well.[31] This value is comparable to that of polytetrafluoroethylene (PTFE), a well-known hydrophobic material. These results suggest the great prospect of −SF_5 as a hydrophobic group. However, detailed insights on its physical parameters are not available, and a direct comparison of the effects of −SF_5 and −CF_3 group-containing compounds on surface properties has not been made. Furthermore, the differences between −SF_5 and −CF_3 group-containing compounds in contact with water are still not sufficiently clarified.

In this study, to experimentally demonstrate the higher hydrophobicity of the −SF_5 groups compared to other reported fluorine-based hydrophobic groups, we investigated the surface free energies and affinities to water of poly(methacrylate) with −SF_5 groups in its side chains, comparing with poly(methacrylate) derivatives containing other functional groups, viz., −CF_3, −CH_3, and −H. We evaluated the dynamic contact angles of water and ethylene glycol on the thin films of poly(methacrylate) derivatives with different functional groups and their neutron reflectivities (NRs) in contact with water.

Experimental

Materials

4-Pentafluorosulfanyl phenol (97%) was purchased from Alfa Aesar. 4-trifluoromethyl phenol (97%) and deuterium oxide (D_2O, 99.9% D) were obtained from Sigma-Aldrich. *p*-Cresol (99.0%), phenyl methacrylate (>88%), tetrahydrofuran (THF, deoxidized, >99.5%), and chloroform (super-dehydrated, >99.0%) were purchased from Wako Pure Chemical Industries, Ltd. Triethylamine (≥99.0%) and 2,2'-azobis(isobutyronitrile) (AIBN, ≥98%) were purchased from Nacarai Tesque, Inc. Methacryloyl chloride (>90%) was purchased from TCI Chemicals. All the chemicals were used without further purification. ^{1}H NMR (400 MHz) measurements were carried out by a JEOL ECZ400 spectrometer in $CDCl_3$. The chemical shifts are expressed in ppm; the signal of $CHCl_3$ (7.26 ppm for ^{1}H) was used as the internal standard. The ^{13}C NMR (100 MHz) measurements in $CDCl_3$ solvents were performed, and the signal of $CDCl_3$ (δ = 77.7 ppm for ^{13}C) was used as the internal standard. ^{19}F NMR (376 MHz) spectra were recorded using hexafluorobenzene (δ = −164.9 ppm for ^{19}F) as the internal standard in $CDCl_3$. To measure the molecular weight and polydispersity of the synthesized polymethacrylates, Gel Permeation Chromatography (GPC) (CBM-20A, Shimadzu) was carried out using a reflectivity index detector at 40 °C. The GPC apparatus consisted of a TSK guide column, HXR-H column, and TSK-gel GMHHR-M column (TOSOH Co., Ltd.). THF was used as the eluent. Before the GPC measurements of the prepared samples, polystyrene samples with different molecular weight (TOSOH Co., Ltd., M_w = 2,630, 9,100, 37,900, 96,400, 190,000 and 355,000) were used as standards for the calibration curve.

Synthesis of monomers and polymers

Synthesis of monomers

Three monomers, 4-pentafluorosulfanylphenyl methacrylate, 4-trifluoromethylphenyl methacrylate, and 4-methylphenyl methacrylate, were synthesized with a similar esterification reaction. The synthetic procedure of 4-pentafluorosulfanylphenyl methacrylate is described as a representative. First, a mixture of 4-pentafluorosulfanyl phenol (1.0 g, 4.5 mmol) and methacryloyl chloride (0.47 g, 4.5 mmol) was dissolved in chloroform (30 mL) under N_2 gas. Then, triethylamine (3.0 mL) was added ito the solution under stirring, and the resulting mixture was stirred further for about 8 hours at room temperature under N_2 gas. The reaction was terminated by letting air into the reactor, and the mixture was washed with H_2O and then a saturated brine solution, three times respectively. After drying over $MgSO_4$, the organic layer was evaporated under reduced pressure, and the residual solid was purified by silica gel column chromatography using hexane/ethyl acetate (1 : 20) as the eluent, and the yield was 69%. ^{1}H NMR (400 MHz, $CDCl_3$) : δ (ppm) = 7.80 (d, J_{HH} = 9.2 Hz, 2H), 7.24 (d, J_{HH} = 9.2 Hz, 2H), 6.38 (s, 1H), 5.82 (t, J_{HH} = 1.4 Hz, 1H), 2.07 (s, 3H). ^{13}C NMR (101 MHz, $CDCl_3$)): 165.2, 152.9, 151.0, 135.4, 128.3, 127.6 (t, J_{CF} = 4.3 Hz), 122.0, 18.4. ^{19}F NMR (282 MHz, $CDCl_3$)): 84.2 (quintet, J_{FF} = 155 Hz), 63.5 (d, J_{FF} = 143 Hz).

4-Trifluoromethylphenyl methacrylate

Yield : 65%. ^{1}H NMR (400 MHz, $CDCl_3$) : δ (ppm) = 7.67 (d, J_{HH} = 9.1 Hz, 2H), 7.25–7.27 (m, 2H), 6.38 (s, 1H), 5.81 (t, J_{HH} = 1.4 Hz, 1H), 2.07 (s, 3H). ^{13}C NMR (101 MHz, $CDCl_3$)): 165.4, 153.6, 135.5, 128.1 (q, J_{CF} = 33 Hz), 128.0, 126.8 (q, J_{CF} = 4 Hz), 125.4, 122.6, 122.2, 119.9, 18.3. ^{19}F NMR (282 MHz, $CDCl_3$)): -62.3.

4-Methylphenyl methacrylate[32]

Yield : 66%. ^{1}H NMR (400 MHz, $CDCl_3$) : δ (ppm) = 7.18 (d, J_{HH} = 8.4 Hz, 2H), 6.99 (d, J_{HH} = 8.0 Hz, 2H), 6.34 (s, 1H), 5.74 (t, J_{HH} = 1.4 Hz, 1H), 2.35 (s, 3H), 2.06 (s, 3H).

Synthesis of polymers

All the monomers were polymerized by the conventional radical polymerization method using AIBN as the initiator. Here, only the synthesis of poly(4-pentafluorosulfanylphenyl methacrylate) ($P(SF_5)$) is described as an example.

Synthesis of $P(SF_5)$

Briefly, 4-pentafluorosulfanylphenyl methacrylate (0.5 g, 1.7 mmol) and AIBN (2.8 mg, 17 μmol (1 mol%)) were first dissolved in THF (10 mL) under N_2 gas. Then, three cycles of freeze-pump-thaw processes were conducted to remove the residual air in the solution and reactor. After stirring at 70 °C for 8 h under N_2 gas, the reaction was terminated by freezing the reactor with liquid N_2. The product was purified by three cycles of reprecipitation from chloroform using hexane as the poor solvent, and the converted sample was dried under vacuum for 1 day. The yield was calculated as 50%. ^{1}H NMR (400 MHz, $CDCl_3$) : δ (ppm) = 7.78–7.57 (br, 2H), 7.21–7.05 (br, 2H), 2.60–1.67 (br, 2H), 1.67–1.18 (br, 3H). ^{13}C NMR (101 MHz, $CDCl_3$)): 174.9, 174.6, 174.2, 174.0, 152.0, 151.5, 151.3, 151.1, 150.9, 127.7, 127.5, 121.8, 121.5, 121.3, 54.7, 54.2, 45.8, 31.7, 22.8, 20.6, 19.4, 19.1, 14.2. ^{19}F NMR (282 MHz, $CDCl_3$)): 82.0-84.5 (br), 63.3 (d, J_{FF} = 143 Hz). M_n : 9.9k, M_w : 12.1k, M_w/M_n : 1.2.

Poly(4-trifluoromethylphenyl methacrylate) ($P(CF_3)$)

Yield : 58%. ^{1}H NMR (400 MHz, $CDCl_3$) : δ (ppm) = 7.63–7.38 (br, 2H), 7.21–7.05 (br, 2H), 2.60–1.67 (br, 2H), 1.67–1.30 (br, 3H). ^{13}C NMR (101 MHz, $CDCl_3$)): 175.1, 174.8, 174.1, 152.8, 128.7, 128.5, 127.0, 126.8, 125.0, 122.3, 121.9, 121.7, 121.5, 45.9, 31.7, 22.8, 20.5, 19.0, 18.9, 14.2. ^{19}F NMR (282 MHz, $CDCl_3$)): -62.4. M_n : 13.0k, M_w : 17.4k, M_w/M_n : 1.3.

Poly(4-methylphenyl methacrylate) (P(CH_3))

Yield : 55%. ^{1}H NMR (400 MHz, $CDCl_3$) : δ (ppm) = 7.16–6.86 (br, 4H), 2.60–1.79 (br, 5H), 1.66–1.30 (br, 3H). ^{13}C NMR (101 MHz, $CDCl_3$)): 176.2, 175.8, 175.6, 175.2, 148.5, 135.6, 130.1, 121.2, 121.0, 120.8, 54.6, 45.9, 45.8, 31.7, 22.8, 21.0, 20.0, 18.2, 14.2. M_n : 6.9k, M_w : 9.3k, M_w/M_n : 1.3.

Poly(phenyl methacrylate) (P(H))

Yield : 54%. ^{1}H NMR (400 MHz, $CDCl_3$) : δ (ppm) = 7.38–6.97 (br, 4H), 2.60–1.79 (br, 2H), 1.70–1.30 (br, 3H). ^{13}C NMR (101 MHz, $CDCl_3$)): 176.0, 175.6, 175.3, 175.0, 150.6, 129.9, 129.6, 129.5, 126.0, 121.6, 121.3, 121.1, 54.6, 46.0, 45.8, 20.0, 18.2. M_n : 5.2k, M_w : 7.5k, M_w/M_n : 1.4.

Film preparation for contact angle measurements and X-ray diffraction measurements

First, 1 wt% THF solutions of the four types of synthesized polymethacrylates were prepared. Then, thin films were fabricated on silicon wafers (20 mm × 20 mm, 625 μm thick) by spin-coating 2 mL of each solution. Spin-coating was performed using a spin coater (ABLE Co., Ltd.) at a rotating speed of 1500 rpm for 12 s to spread the solution over the silicon wafer, followed by 3000 rpm for 48 s. The films were dried overnight at room temperature after coating.

X-ray diffraction measurements of thin films

Small angle incidence X-ray diffraction measurements were performed with SmartLab (Rigaku Co.) with 30 mA and 40 kV. The CuKα X-ray beam (wavelength of 1.5418 Å) was irradiated on the surface with the incident angle of 0.20°, which is larger than the critical angles of the synthesized polymers. The detector of X-ray beam was a scintillation counter. The detector scanned in the out-of-plane direction. The small angle incidence X-ray diffraction measurements were performed with larger incident angle of X-ray beam than the critical angle. Therefore, the bulk structures of the thin films were investigated with large footprints.

Thermogravimetric analysis (TGA) and differential scanning calorimetry (DSC)

Thermogravimetry (Thermo Plus EVO2, Rigaku Co. Ltd.) was performed at a heating rate of 10 °C/min under N_2 flow. The temperature with 5% thermal weight loss (T_{d5}) is defined as the thermal decomposition temperature. The glass transition temperatures (T_g) of all the polymethacrylate derivatives were measured by DSC. T_g was defined as the temperature at which the baseline changes during the heating process. DSC profiles were recorded using a Rigaku DSC8230 with 5 mg of the sample at the scan rate of 10 °C/min under dried N_2.

X-ray photoelectron spectroscopy (XPS)

XPS measurements were carried out using an ULVAC-PHI PHI X-tool-F instrument to investigate the chemical composition of the surfaces. Al $K\alpha$ radiation generated at 15 kV and 0.26 mA was irradiated on the samples.

Dynamic contact angle

To investigate the wettability of each film, the dynamic contact angles of deionized water and ethylene glycol were measured at room temperature. The advancing contact angle (θ_a) was measured while the droplet (<1 mm in diameter) was enlarged (<2 mm in diameter) upon injecting the liquid from a microsyringe onto the film surface until the contact area increased. The receding contact angle (θ_r) was measured when the contact area decreased by withdrawing the liquid slowly. An average of 15 measurements were performed on different locations of the film surface for each liquid, and the average value is reported.

In order to evaluate the wettability of the film surface, the average contact angle (θ_{av}) was calculated using Eq. (1)

$$\theta_{av} = \arccos[(\cos\theta_a + \cos\theta_r)\ /2] \quad (1)$$

The surface free energy, γ_s was calculated from the contact angles, using Eq. (2) and (3).[33,34]

$$(1 + \cos\theta_{av}) \times \gamma_L / 2 = \sqrt{\gamma_S{}^d \times \gamma_L{}^d} + \sqrt{\gamma_S{}^p \times \gamma_L{}^p} \quad (2)$$

$$\gamma_s = \gamma_s{}^d + \gamma_s{}^p \quad (3)$$

where γ_L is the surface free energy of the liquid, and $\gamma_L{}^d$ and $\gamma_L{}^p$ are the dispersion and polar components of the liquid, respectively. The $\gamma_L{}^d$ and $\gamma_L{}^p$ values of water are 21.8 and 51.0 mJ/m^2 , respectively and those of ethylene glycol are 29.3 and 19.0 mJ/m^2, respectively.[35] $\gamma_s{}^d$ and $\gamma_s{}^p$ are the dispersion and polar components of the surface, respectively.

NR measurements

Sample preparation

The thin films for NR experiments were fabricated from 1 wt% THF solutions of the four types of polymethacrylates in the spin-coating method. Cylindrical silicon blocks with a diameter of 76 mm and height of 10 mm were used as substrates. The rotating speed during the process was set to 1000 rpm for 60 s. All film samples were dried at room temperature overnight after fabrication.

After the initial NR measurement in air, NR measurements was performed in water to investigate the structural changes in each film in contact with water and discuss the affinity between each polymer and water. In these experiments, pure D_2O or a D_2O/H_2O mixture (D_2O:H_2O = ~7:3) was employed instead of H_2O for a clear contrast with the polymers. After the measurement in air, the same samples were sandwiched between two pieces of metal plates, and D_2O or the D_2O/H_2O mixture was injected from a spout on the top of the upper metal plate. The samples in contact with water were left to stand for more than 2 h before the measurement which is sufficient for equilibration, as reported.[36]

Measuring apparatus and conditions

The NR measurement was carried out at 25 °C with a Soft Interface Analyzer (SOFIA, BL-16, Materials and Life Science Facility (MLF), Japan Proton Accelerator Research Complex (J-PARC)).[37,38] Neutron beams with wavelengths ranging from 0.20 to 0.88 nm were irradiated onto the film from the air side for the measurements in air and from the substrate side for measurements in D_2O. The q range in the NR measurements was from 0.01 to 0.16 $Å^{-1}$. The incident angles of the neutron beams were 0.30°, 0.75° and 1.80°. MOTOFIT software was used to fit the experimental results. Global fitting was performed on the NR profiles of the polymer thin films in contact with D_2O and D_2O/H_2O. In the global fitting, the thickness, volume fraction of water and roughness at every layer of the polymer thin film in contact with water were linked. In the fitting process, the scattering length density (SLD) of the polymer in air was employed as the SLD of the polymer layers in contact with water.

Results and Discussion

Four polymethacrylate derivatives with different side chains, viz., P(SF_5), P(CF_3), P(CH_3), and P(H) with $-SF_5$, $-CF_3$, $-CH_3$, and –H in their side chains, respectively, through conventional radical polymerization in 50 to 60% yields, as shown in Figure 1. The obtained polymers were characterized by ^{1}H, ^{13}C, and ^{19}F NMR spectroscopies and their molecular weights were estimated using GPC. In their NMR spectra as shown in Figure S1–S17 in the Supporting Information, all the peaks were assigned. In the ^{19}F NMR spectrum of P(SF_5), the two peaks at 63 and 83 ppm were assigned to fluorine atoms at the equatorial and axial positions of the $-SF_5$ groups, respectively. The peak positions were similar to those of the monomer. This indicates that the $-SF_5$ group has high stability and durability toward radical polymerization and purification processes. In addition, the weight-average molecular weights of the synthesized polymers ranged from 7.5k to 17.4k. These molecular weights are suitable for solubilizing them in conventional organic solvents for spin-coating thin films to evaluate their surface properties and structures. For the investigation of the crystallinity of their thin films, we performed X-ray diffraction measurements. The diffraction profiles of their polymers are shown in Figure 2a. In the profiles of the thin films of all the polymers, there were only amorphous halos, not diffraction peaks, which meant that the synthesized polymers were amorphous. The thermal properties of the polymers were evaluated by TGA and DSC measurements. The decomposition temperatures of the synthesized polymers, T_{d5}, at which 5% mass was lost during heating, are presented in Table 1 and Figure S18 in the Supporting Information. The T_{d5} of P(SF_5) was higher than 250 °C, and comparable to that of P(CF_3). This result suggested that the $-SF_5$ group possessed sufficient thermal stability to be used in various circumstances, as it does not decompose of at around 200 °C. In DSC thermograms of all the polymers in Figure 2b, the endothermic peaks of melting points were not observed. These results

corresponded to those of X-ray diffraction measurements. In addition, the DSC measurements revealed the glass transition temperature (T_g) of P(SF_5) to be 134 °C, being higher than those of the other synthesized polymers, as shown in Table 1. The reason is for the bulky structure and polarity of the $-SF_5$ groups in its side chains. Actually, it is estimated that the volume and electronegativity of the $-SF_5$ group were 49.20 cm^3/mol and 3.65, which were larger than 20.49 cm^3/mol and 3.36 of a $-CF_3$ group.[27,39–42]

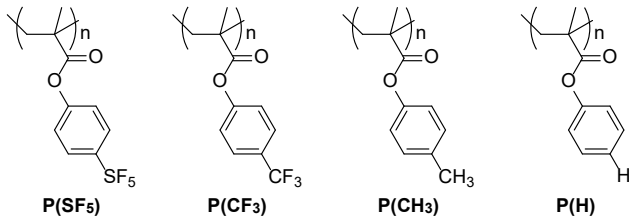

Figure 1. Chemical structures of the synthesized polymethacrylates.

Table 1. Thermal decomposition temperatures (T_{d5}) and glass transition temperatures (T_g) of the synthesized polymethacrylates.

Sample	T_{d5}	T_g
	°C	°C
P(SF_5)	276	134
P(CF_3)	278	77
P(CH_3)	216	83
P(H)	190	53

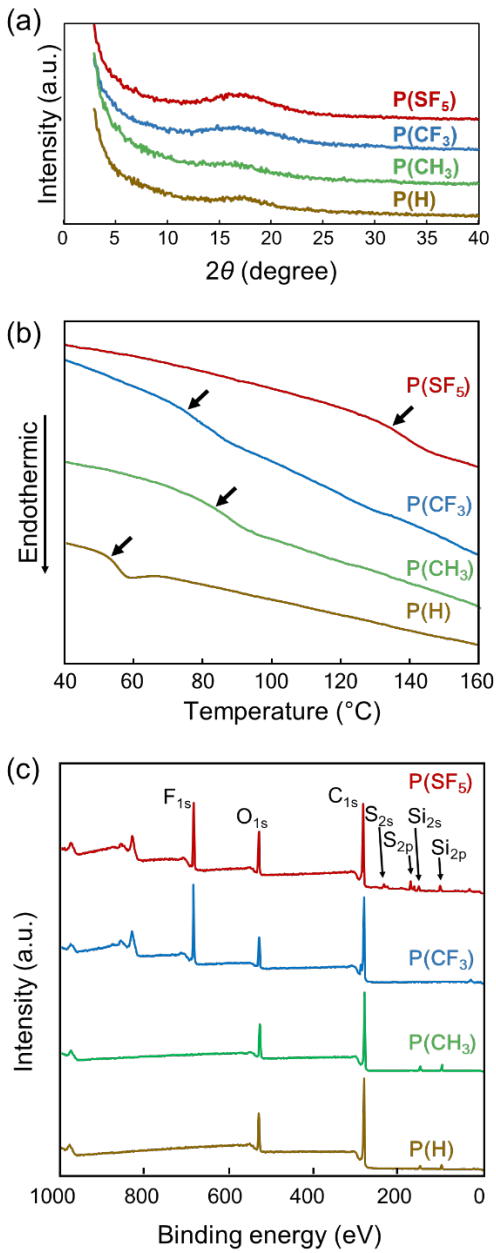

Figure 2. (a) X-ray diffraction profiles, (b) DSC thermograms and (c) XPS profiles of $P(SF_5)$, $P(CF_3)$, $P(CH_3)$, and P(H).

Thin flat films were prepared on silicon wafers/blocks in spin-coating methods using a 1 wt% THF solution of the synthesized polymers for the measurements of dynamic contact angles and NR. The XPS profiles exhibited peaks from all the elements in their synthesized polymer structures,

as shown in Figure 2c. In the XPS profile of P(SF_5) and P(CF_3), F_{1s} peaks were observed at 687 and 688 eV, respectively. In addition, two S_{1p} peaks were detected at 172 and 164 eV for P(SF_5), corresponding to the bonding of S with F atoms at the equatorial and axial positions in the $-SF_5$ group.

Table 2. Dynamic contact angles and surface free energies of the four spin-coated films.

Sample	Dynamic contact angle θ_{av}		Surface free energy		
	Water	Ethylene glycol	γ^d	γ^p	γ
	degree		mJ/m^2		
P(SF_5)	102 ± 1	85 ± 2	11.8	3.1	15.0
P(CF_3)	96 ± 1	73 ± 2	19.7	2.7	22.4
P(CH_3)	92 ± 2	68 ± 5	20.9	3.8	24.7
P(H)	81 ± 2	57 ± 2	21.0	8.3	29.3

γ^d : Dispersion component of the surface free energy. γ^p : Polar component of the surface free energy. : Total surface free energy.

For the investigation on the surface properties, we measured dynamic contact angles of water and ethylene glycol droplets on the prepared thin films and calculated the surface free energies of their polymers.[33–35] Table 2 shows dynamic contact angles of water and ethylene glycol droplets on the polymer surface along with their surface free energies of the polymers and their components of dispersion γ^d and polar γ^p components. The advancing and receding contact angles of water and ethylene glycol droplets are listed in Table S2 in the Supporting Information. The polymer thin films containing fluorinated groups in their side chains possessed higher dynamic contact angles of water and ethylene glycol droplets; that is, they had lower surface free energies than the thin films of the obtained polymers without any fluorine atoms in their side chains. The thin films of

P(SF_5) and P(CF_3) exhibited larger contact angles for both liquids. It is revealed that both the hydrophobicity and oleophobicity of P(SF_5) and P(CF_3) were higher than those of P(CH_3) and P(H). In particular, P(SF_5) represented the largest dynamic contact angles of water and ethylene glycol droplets and the lowest surface free energy, which implies that it has the highest hydrophobicity and oleophobicity of P(SF_5) among the synthesized polymers. In the components of their surface free energies, the polar components γ^p were lower for the two polymers with fluorine side chains, while the dispersion component γ^d of P(SF_5) was declined relative to those of the other polymers including P(CF_3). These results unequivocally suggest that P(SF_5) has the lowest surface free energy. Thus, the larger the number of fluorine atoms in the functional group is, the lower the surface free energy is and hence higher the hydrophobicity is.

It is worth noting that the surface free energies of P(SF_5) and P(CF_3) are however larger than those of polymethacrylates with perfluoroalkyl side chains.[43–48] The latter surface free energies were lower than 10 mJ/m^2. The reason is that the volume fractions of the perfluoroalkyl groups are larger than those of P(SF_5) and P(CF_3), and the perfluoroalkyl side chains self-assemble and align at the surface, because of the rigid structure originated from larger fluorine atoms than hydrogen. Further appropriate molecular designs for the backbone of $-SF_5$ groups could lead to much more hydrophobic properties and lower surface free energies.

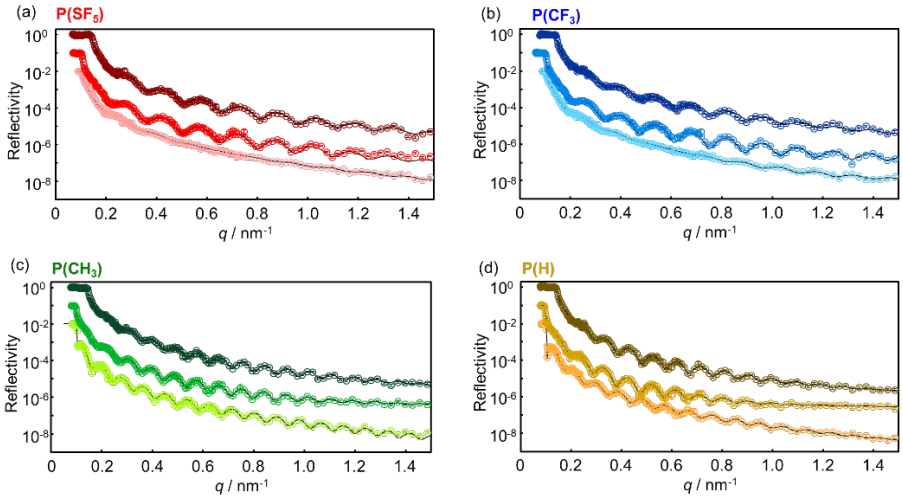

Figure 3. Neutron reflectivity profiles (circles) of the spin-coated films of (a) $P(SF_5)$, (b) $P(CF_3)$, (c) $P(CH_3)$, and (d) P(H) in contact with air (bottom) and D_2O (upper) and D_2O/H_2O (middle), and the fits (lines) using a single layer or double-layer model for air, and double- or triple-layer model. For clarity, the curves are offset by a decade.

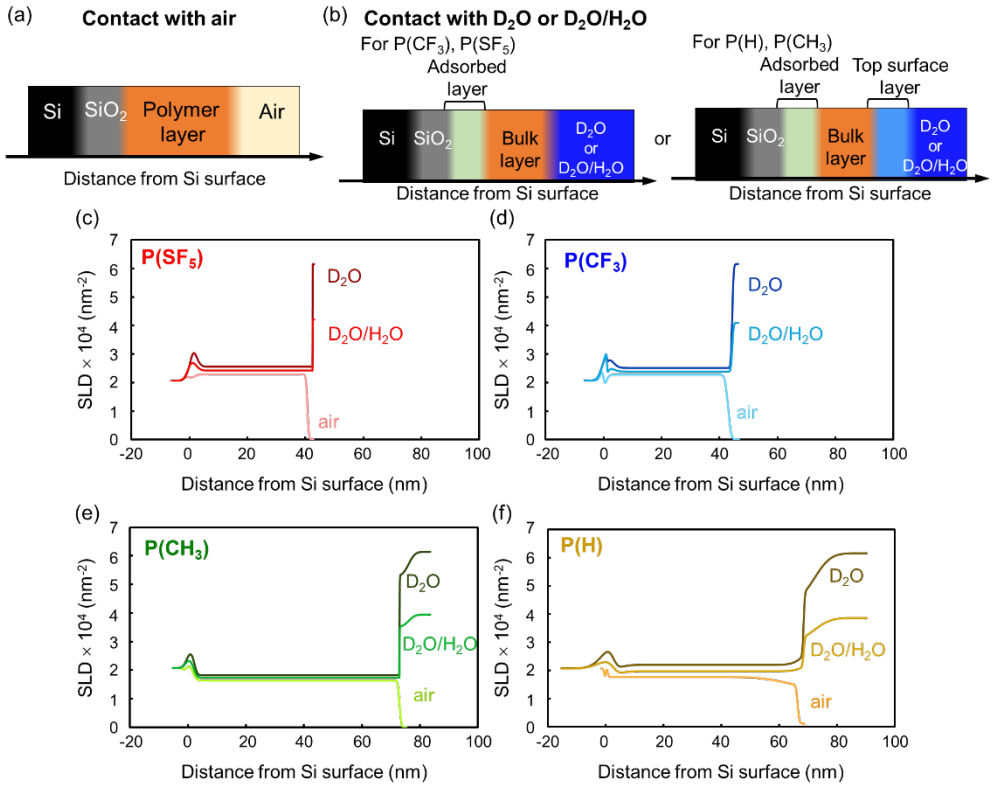

Figure 4. Fitting models of polymer thin films in contact with (a) air and (b) D_2O or D_2O/H_2O. SLD profiles of the spin-coated films of (c) P(SF_5), (d) P(CF_3), (e) P(CH_3), and (f) P(H) in air, D_2O, and D_2O/H_2O.

For a detailed analysis of the affinity of the polymer P(SF_5) to water, we performed NR measurements of the spin-coated thin films in contact with air, deuterated water (D_2O), and D_2O/H_2O mixture at SOFIA (BL-16, MLF, J-PARC)[37,38] and evaluated the structures of the thin films at 25 °C. The NR profiles and the corresponding fits are shown in Figure 3. The smaller Kiessig fringes were observed in the NR profiles of P(SF_5) and P(CF_3) in the contact with air, relative to P(CH_3) and P(H), because the SLD values of P(SF_5) and P(CF_3) were similar to the SLD value of the silicon substrate. In the fitting of all the thin films, except that of P(H), in contact with air, we could analyze the observed NR profiles of the thin films as single polymer layer model, as shown in Figure 4a. This fitting model consists of air, the polymer layer, the natural oxidized layer (SiO_2) and the silicon substrate, along the pathway of the incident neutron beam. On the contrary, for the P(H) in contact with air, its NR profile fitting analysis fitted better with the double-layer model, rather than single-layer model. The structural parameters, including the thickness, roughness, and SLD values were estimated from the fitting curves, as shown in Table S3 in the Supporting Information. The thickness of these polymer thin films ranged from 40 to 75 nm, and the roughness was less than 1 nm for all cases. The low surface roughness of these polymer films would exclude its effect on dynamic contact angle. From the NR results, it is concluded that the smooth thin films were prepared and the reasonable values of thickness and SLD of their thin films were obtained.

For the evaluation of the interactions between the synthesized polymers and water, we measured NRs of the polymer films in contact with D_2O, and D_2O/H_2O (D_2O:H_2O volume ratio = 7:3). As shown in Figure 3, the contact with D_2O or D_2O/H_2O and polymer thin films provided clear Kiessig fringes in the NR profiles because of the large difference in the SLD values of the polymer thin films and D_2O or D_2O/H_2O. The polymer layers in the fitting models illustrated in Figure 4b are composed of an adsorbed layer and a bulk layer for P(CF_3) and P(SF_5), or a water-adsorbed layer (ads), a polymer bulk layer (bulk), and a top surface layer (top) for P(H) and P(CH_3), from interface with the silicon wafer substrate, that is, the neutron beam incidence side.[36,49] The fitting analyses were performed via global fitting of the obtained NR profiles of all the polymers in contact with D_2O and D_2O/H_2O. For global fitting, we assumed that the thickness, volume fraction of water and roughness at each layer had no difference between the polymer thin films in contact with D_2O and D_2O/H_2O. In addition, the volume fractions of water in the polymer thin films in contact with water were calculated using the SLD values of the polymers in contact with air.

The fitting parameters of the four thin polymer films in contact with water are listed in Table S4 in the Supporting Information. In Figure 4c-4f, SLD profiles of the polymers in contact with air, D_2O, and D_2O/H_2O mixture are summarized. Table 3 shows the thickness and SLD of the polymer thin films under air atmosphere, and thickness, volume fraction of water, values of the films and roughness in contact with water. The NR profiles of P(CF_3) and P(SF_5) were fitted with the double-layer model, while those of P(H) and P(CH_3) were fitted with the triple-layer model.

Table 3. Thickness, SLD, and volume fractions of water of P(SF_5), P(CF_3), P(CH_3), and P(H) thin films in contact with air and D_2O or D_2O/H_2O.

Sample	t_{air}[a]	SLD_{air}[b]	t_{ads}[c]	t_{blk}[c]	t_{top}[c]	Φ_{ads}[d]	Φ_{blk}[d]	Φ_{top}[d]	R_{top}[e]
	nm	$\times 10^{-4}$ nm^{-2}	nm	nm	nm	vol%	vol%	vol%	nm
P(SF_5)	40.8 ± 0.2	2.29 ± 0.00	0.6 ± 0.2	41.1 ± 0.3	—	56.2 ± 7.9	7.0 ± 0.3	—	<0.1 ± 2.7
P(CF_3)	43.0 ± 0.1	2.28 ± 0.00	1.4 ± 0.4	41.9 ± 0.5	—	22.3 ± 2.7	6.1 ± 0.3	—	0.4 ± 0.0
P(CH_3)	72.4 ± 0.3	1.63 ± 0.00	1.7 ± 1.3	70.8 ± 0.6	3.1 ± 1.8	20.1 ±12.6	3.9 ± 0.3	81.1 ±17.9	1.7 ± 0.9
P(H)	66.3 ± 2.6[f]	1.77 ± 0.01[g]	2.2 ± 0.2	66.0 ± 0.1	3.8 ± 0.5	34.6 ± 2.4	9.8 ± 0.6	60.2 ± 2.3	4.4 ± 0.3

[a] Thickness of the polymer layer in contact with air.
[b] SLD of the polymer layer in contact with air.
[c] Thicknesses of the adsorbed layer (t_{ads}), bulk layer (t_{blk}), and top surface layer (t_{top}) in contact with water.
[d] Volume fractions of water in the adsorbed layer, bulk layer (Φ_{blk}), and top surface layer (Φ_{top}) in contact with water, for Φ_{ads}, Φ_{blk}, and Φ_{top}, respectively. Φ_x is defined as Φ_x (%) = 100 × (volume of water)$_x$ / [(volume of water)$_x$ + (volume of polymer)$_x$]. Φ_x was calculated using relationship: $SLD_x = [\Phi_x \times SLD_{water} + (100 - \Phi_x) \times SLD_{air}] / 100$.
[e] Roughness of the surface in contact with water.
[f] Total thickness of bulk layer 1 and bulk layer 2, as shown in Table S3 in the Supporting Information.
[g] SLD of the main bulk layer 1, as shown in Table S3 in the Supporting Information.

The total thickness of all the polymer films were increased in the contact with water (D_2O or D_2O/H_2O), indicating that all of them included water. The reason is that water molecules penetrated the thin films. In the water-adsorbed layers, a number of water molecules aggregated and formed ultra-thin layers at the interface between the polymer and substrate.[36,50] For proof of the formation of the water-adsorbed layers, we performed fitting analyses, assuming that these layers were composed of only aggregated polymer chains.[51,52] The SLD values of the adsorbed layers, SLD_{ads}, in contact with D_2O and D_2O/H_2O were clearly different; the SLD_{ads} value obtained with D_2O was larger than that obtained with D_2O/H_2O. In the case of aggregation of polymer chains, both the SLD_{ads} values in the contact with D_2O and D_2O/H_2O would be same. These results indicated that the adsorbed water layer would be formed at the interface between the polymer film and substrate.

For the discussion of the surface properties of the polymer thin films, we focused on the top surface layers in the triple-layer fitting model and the surface roughness in the double-layer fitting model. According to the fitting results, the uppermost surface regions of P(H) and P(CH_3) contained much larger volume fractions of water, Φ_{top}, relative to those in the bulk layers. As the Φ_{top} values decrease to 0 vol%, the top surface layer is composed of only polymer chains, while, with an increase of Φ_{top} to 100%, a layer composed of only water is formed. The volume fractions of the polymers at the top surface layers of P(H) and P(CH_3) were 40% and 19%, respectively. In the thin films of P(H) and P(CH_3), polymer chains and water were mixed at the top surface layers. Next, the global fitting for NR profiles of P(SF_5) and P(CF_3) in contact with water was performed using the double-layer model without a top surface layer and the better results for NR profiles of P(CF_3) and P(SF_5) were obtained relative to those using the triple-layer model. The lower affinity of P(CF_3) and P(SF_5) toward water were clarified through these fitting into the double-layer model. In the P(CF_3) film, the roughness at the interface between the bulk layer and water increased. This suggested that the narrow surface region was slightly swollen. On the other hand, for the P(SF_5) thin film, the roughness of the top surface in contact with water was very slight, indicating that there was little affinity between the top surface of this film and water. These results mean that the top surface regions of the P(H) and P(CH_3) thin films were swollen significantly by water because of the stronger interaction of the polymer chains with water. Meanwhile, the polymer chains at the top surface of P(CF_3) were swollen only slightly, whereas the surface of P(SF_5) did not possess swollen polymer chains, as shown in Figure 5.

The global fitting for the NR profiles of P(SF_5) and P(CF_3) in contact with water was also performed using the triple-layer model with a top surface layer. The fitting results for NR profiles of P(SF_5) and P(CF_3) are shown and summarized in Figure S19 and S20, and Table S5 and S6 in

the Supporting Information. P(SF_5) showed abrupt changes in the SLD at the interface between the bulk and top surface layer, and the surface layer was composed of almost only water because the value of Φ_{top} was >99%. In the case of P(CF_3), the SLD changed substantially at the interface between the bulk and top surface layer, but a small number of polymer chains were included in the top surface layer. These results correspond to the fitting parameters from double-layer model.

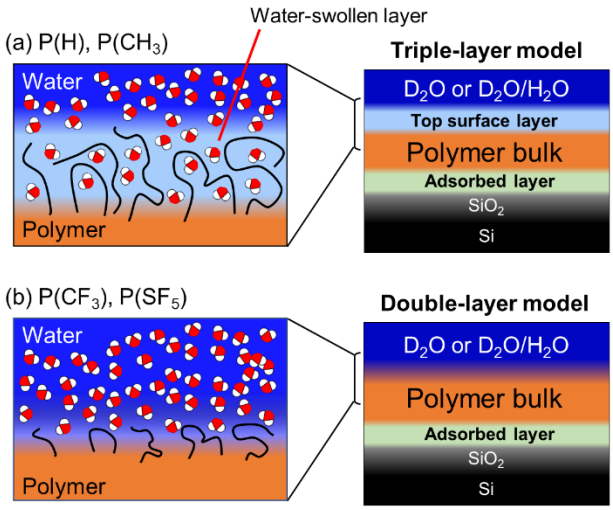

Figure 5. Schematic models of the surfaces of thin films of (a) P(H) and P(CH_3) (b) P(CF_3) and P(SF_5) in contact with water.

From these comparisons of the top surfaces of the polymer films in contact with water, it is revealed that the affinity of the surface of P(SF_5) to water was the lowest among these examined polymers. These results corresponded to the hydrophobicity and surface free energies of their polymers. These suggested that water-affinity and hydrophobicity of the polymer thin films were evaluated by analyzing the topmost surfaces of the polymer thin films at the molecular scale through NR measurements and analyses. Moreover, $-SF_5$ group itself possesses hydrophobicity, which leads to hydrophobic property at the macro scale. It is suspected that appropriate alignment

of the $-SF_5$ group at the surface might provide higher hydrophobicity beyond trifluoromethyl $-CF_3$ group.

CONCLUSIONS

We investigated the hydrophobic properties of the $-SF_5$ group through the evaluation of its surface contact angle and neutron reflectivity. The polymethacrylates with $-SF_5$ groups and other functional groups in their side chains were synthesized and characterized, and thin films were prepared by spin coating. The $-SF_5$ groups possessed durability against thermal and radical under reaction. The synthesized polymer with $-SF_5$ groups in side chain was amorphous, corresponding to the other synthesized polymethacrylates. The glass temperature of the polymer with $-SF_5$ groups was more than 130 °C, the highest among all the synthesized polymers. This highest glass transition temperature was originated from the bulky structure and polarity of the $-SF_5$ groups. The contact angle measurements of water and ethylene glycol on the thin films were performed and their surface free energies were calculated. The surface free energy of the polymethacrylate film with $-SF_5$ groups was lower than those of the other polymer thin films, and its hydrophobicity was the largest. Moreover, the neutron reflectivity measurements and analyses of the polymer thin films in contact with water were performed. The polymethacrylate film with $-SF_5$ and $-CF_3$ groups in the contact with water formed no swollen top surface layer, whereas the polymer without fluorine groups possessed the swollen layers at the top surface. In addition, the sharpness of the interface of the polymethacrylates with $-SF_5$ groups with water was increased, relative to that of the polymethacrylates with $-CF_3$ groups. These results proved that the $-SF_5$ group possessed lower affinity toward water than the other synthesized polymers and the lower affinity of $-SF_5$ groups directly connected to hydrophobicity of the polymethacrylates with $-SF_5$ groups. The $-SF_5$ group is an inherently promising chemical entity for developing hydrophobic materials.

ASSOCIATED CONTENT

Supplementary Data.

This material included ^{1}H, ^{13}C, and ^{19}F NMR spectra, molecular weight and polydispersity, thermogravimetric trace curves, advanced, receding and averaged dynamic contact angles and surface free energies, fitting parameters for NR profiles in the contact with air and water, fitting profiles and parameters for NR profiles of $P(SF_5)$ and $P(CF_3)$ in the contact with air and water using triple-layer models. The Supporting Information data file is available free of charge via the Internet at http://

AUTHOR INFORMATION

Corresponding Author

*(T.N.) E-mail: tnishino@kobe-u.ac.jp

*(T.M.) E-mail: matsumoto0521@person.kobe-u.ac.jp

Author Contributions

The manuscript was written through contributions of all authors. All authors have given approval to the final version of the manuscript.

Funding Sources

The neutron experiment at the Materials and Life Science Experimental Facility (MLF) of J-PARC was performed under the user program (Proposal No. 2018A0219). This work was supported by JSPS KAKENHI Grant Number JP22H04546, JP20H05222, and JP19H05717.

Acknowledgements

We would like to thank Editage (www.editage.com) for English language editing.

Notes

The authors declare no competing financial interest.

REFERENCES

(1) Lu, Y.; Sathasivam, S.; Song, J.; Crick, C. R.; Carmalt, C. J.; Parkin, I. P. Robust Self-Cleaning Surfaces That Function When Exposed to Either Air or Oil. *Science* **2015**, *347* (6226), 1132–1135. https://doi.org/10.1126/science.aaa0946.

(2) Genzer, J.; Efimenko, K. Recent Developments in Superhydrophobic Surfaces and Their Relevance to Marine Fouling: A Review. *Biofouling* **2006**, *22* (5), 339–360. https://doi.org/10.1080/08927010600980223.

(3) Rosenhahn, A.; Schilp, S.; Kreuzer, H. J.; Grunze, M. The Role of "Inert" Surface Chemistry in Marine Biofouling Prevention. *Phys. Chem. Chem. Phys.* **2010**, *12* (17), 4275–4286. https://doi.org/10.1039/C001968M.

(4) Wang, S.; Yu, X.; Zhang, Y. Large-Scale Fabrication of Translucent, Stretchable and Durable Superhydrophobic Composite Films. *J. Mater. Chem. A* **2017**, *5* (45), 23489–23496. https://doi.org/10.1039/C7TA08203G.

(5) Golovin, K.; Boban, M.; Mabry, J. M.; Tuteja, A. Designing Self-Healing Superhydrophobic Surfaces with Exceptional Mechanical Durability. *ACS Appl. Mater. Interfaces* **2017**, *9* (12), 11212–11223. https://doi.org/10.1021/acsami.6b15491.

(6) Cao, M.; Guo, D.; Yu, C.; Li, K.; Liu, M.; Jiang, L. Water-Repellent Properties of Superhydrophobic and Lubricant-Infused "Slippery" Surfaces: A Brief Study on the Functions and Applications. *ACS Appl. Mater. Interfaces* **2016**, *8* (6), 3615–3623. https://doi.org/10.1021/acsami.5b07881.

(7) Zhang, H.; Chiao, M. Anti-Fouling Coatings of Poly(Dimethylsiloxane) Devices for Biological and Biomedical Applications. *J. Med. Biol. Eng.* **2015**, *35* (2), 143–155. https://doi.org/10.1007/s40846-015-0029-4.

(8) Ozcan, S.; Kaner, P.; Thomas, D.; Cebe, P.; Asatekin, A. Hydrophobic Antifouling Electrospun Mats from Zwitterionic Amphiphilic Copolymers. *ACS Appl. Mater. Interfaces* **2018**, *10* (21), 18300–18309. https://doi.org/10.1021/acsami.8b03268.

(9) Wang, N.; Xiong, D.; Deng, Y.; Shi, Y.; Wang, K. Mechanically Robust Superhydrophobic Steel Surface with Anti-Icing, UV-Durability, and Corrosion Resistance Properties. *ACS Appl. Mater. Interfaces* **2015**, *7* (11), 6260–6272. https://doi.org/10.1021/acsami.5b00558.

(10) Fu, Q.; Wu, X.; Kumar, D.; Ho, J. W. C.; Kanhere, P. D.; Srikanth, N.; Liu, E.; Wilson, P.; Chen, Z. Development of Sol–Gel Icephobic Coatings: Effect of Surface Roughness and Surface Energy. *ACS Appl. Mater. Interfaces* **2014**, *6* (23), 20685–20692. https://doi.org/10.1021/am504348x.

(11) Lacour, S. P.; Courtine, G.; Guck, J. Materials and Technologies for Soft Implantable Neuroprostheses. *Nat. Rev. Mater.* **2016**, *1*, 16063.

(12) Barthwal, S.; Kim, Y. S.; Lim, S.-H. Mechanically Robust Superamphiphobic Aluminum Surface with Nanopore-Embedded Microtexture. *Langmuir* **2013**, *29* (38), 11966–11974. https://doi.org/10.1021/la402600h.

(13) Anton, D. Surface-Fluorinated Coatings. *Adv. Mater.* **1998**, *10* (15), 1197–1205. https://doi.org/10.1002/(SICI)1521-4095(199810)10:15<1197::AID-ADMA1197>3.0.CO;2-F.

(14) Puts, G. J.; Crouse, P.; Ameduri, B. M. Polytetrafluoroethylene: Synthesis and Characterization of the Original Extreme Polymer. *Chem. Rev.* **2019**, *119* (3), 1763–1805. https://doi.org/10.1021/acs.chemrev.8b00458.

(15) Tehrani-Bagha, A. R. Waterproof Breathable Layers – A Review. *Adv. Colloid Interface Sci.* **2019**, *268*, 114–135. https://doi.org/https://doi.org/10.1016/j.cis.2019.03.006.

(16) Mahltig, B.; Böttcher, H. Modified Silica Sol Coatings for Water-Repellent Textiles. *J. Sol-Gel Sci. Technol.* **2003**, *27* (1), 43–52. https://doi.org/10.1023/A:1022627926243.

(17) Gan, D.; Mueller, A.; Wooley, K. L. Amphiphilic and Hydrophobic Surface Patterns Generated from Hyperbranched Fluoropolymer/Linear Polymer Networks: Minimally Adhesive Coatings via the Crosslinking of Hyperbranched Fluoropolymers. *J. Polym. Sci. Part A Polym. Chem.* **2003**, *41* (22), 3531–3540. https://doi.org/10.1002/pola.10968.

(18) Zhang, Y.-X.; Da, A.-H.; Butler, G. B.; Hogen-Esch, T. E. A Fluorine-Containing Hydrophobically Associating Polymer. I. Synthesis and Solution Properties of Copolymers of Acrylamide and Fluorine-Containing Acrylates or Methacrylates. *J. Polym. Sci. Part A Polym. Chem.* **1992**, *30* (7), 1383–1391. https://doi.org/10.1002/pola.1992.080300717.

(19) Coulson, S. R.; Woodward, I. S.; Badyal, J. P. S.; Brewer, S. A.; Willis, C. Ultralow Surface Energy Plasma Polymer Films. *Chem. Mater.* **2000**, *12* (7), 2031–2038. https://doi.org/10.1021/cm000193p.

(20) Schulman, F.; Zisman, W. A. The Spreading of Liquids on Low-Energy Surfaces. V. Perfluorodecanoic Acid Monolayers. *J. Colloid Sci.* **1952**, *7* (5), 465–481. https://doi.org/https://doi.org/10.1016/0095-8522(52)90030-5.

(21) Hare, E. F.; Shafrin, E. G.; Zisman, W. A. Properties of Films of Adsorbed Fluorinated Acids. *J. Phys. Chem.* **1954**, *58* (3), 236–239. https://doi.org/10.1021/j150513a011.

(22) Nishino, T.; Meguro, M.; Nakamae, K.; Matsushita, M.; Ueda, Y. The Lowest Surface Free Energy Based on −CF3 Alignment. *Langmuir* **1999**, *15* (13), 4321–4323. https://doi.org/10.1021/la981727s.

(23) Pitts, C. R.; Bornemann, D.; Liebing, P.; Santschi, N.; Togni, A. Making the SF5 Group More Accessible: A Gas-Reagent-Free Approach to Aryl Tetrafluoro-Λ6-Sulfanyl Chlorides. *Angew. Chemie Int. Ed.* **2019**, *58* (7), 1950–1954. https://doi.org/10.1002/anie.201812356.

(24) Savoie, P. R.; Welch, J. T. Preparation and Utility of Organic Pentafluorosulfanyl-Containing Compounds. *Chem. Rev.* **2015**, *115* (2), 1130–1190. https://doi.org/10.1021/cr500336u.

(25) Kostov, G.; Ameduri, B.; Sergeeva, T.; Dolbier W. R.; Winter, R.; Gard, G. L. Original SF5-Containing Fluorinated Copolymers Based on Vinylidene Fluoride. *Macromolecules* **2005**, *38* (20), 8316–8326. https://doi.org/10.1021/ma0512253.

(26) Altomonte, S.; Zanda, M. Synthetic Chemistry and Biological Activity of Pentafluorosulphanyl (SF5) Organic Molecules. *J. Fluor. Chem.* **2012**, *143*, 57–93. https://doi.org/https://doi.org/10.1016/j.jfluchem.2012.06.030.

(27) Sæthre, L. J.; Berrah, N.; Bozek, J. D.; Børve, K. J.; Carroll, T. X.; Kukk, E.; Gard, G. L.; Winter, R.; Thomas, T. D. Chemical Insights from High-Resolution X-Ray Photoelectron Spectroscopy and Ab Initio Theory: Propyne, Trifluoropropyne, and Ethynylsulfur Pentafluoride. *J. Am. Chem. Soc.* **2001**, *123* (43), 10729–10737. https://doi.org/10.1021/ja016395j.

(28) Hansch, C.; Muir, R. M.; Fujita, T.; Maloney, P. P.; Geiger, F.; Streich, M. The Correlation of Biological Activity of Plant Growth Regulators and Chloromycetin

Derivatives with Hammett Constants and Partition Coefficients. *J. Am. Chem. Soc.* **1963**, *85* (18), 2817–2824. https://doi.org/10.1021/ja00901a033.

(29) Jackson, D. A.; Mabury, S. A. Environmental Properties of Pentafluorosulfanyl Compounds: Physical Properties and Photodegradation. *Environ. Toxicol. Chem.* **2009**, *28* (9), 1866–1873. https://doi.org/10.1897/09-037.1.

(30) Winter, R.; Nixon, P. G.; Gard, G. L.; Graham, D. J.; Castner, D. G.; Holcomb, N. R.; Grainger, D. W. Self-Assembled Organic Monolayers Terminated in Perfluoroalkyl Pentafluoro-Λ6-Sulfanyl (-SF5) Chemistry on Gold. *Langmuir* **2004**, *20* (14), 5776–5781. https://doi.org/10.1021/la040011w.

(31) Winter, R.; Nixon, P. G.; Terjeson, R. J.; Mohtasham, J.; Holcomb, N. R.; Grainger, D. W.; Graham, D.; Castner, D. G.; Gard, G. L. Perfluorinated Polymer Surfaces Comprising SF5-Terminated Long-Chain Perfluoroacrylate. *J. Fluor. Chem.* **2002**, *115* (2), 107–113. https://doi.org/https://doi.org/10.1016/S0022-1139(02)00008-8.

(32) Grigg, R.; Monteith, M.; Sridharan, V.; Terrier, C. Palladium Catalysed Reactions of Allenes, Carbon Monoxide and Nucleophiles. *Tetrahedron* **1998**, *54* (15), 3885–3894. https://doi.org/https://doi.org/10.1016/S0040-4020(98)00115-X.

(33) Fowkes, F. M. Additivity of Intermolecular Forces at Interfaces. I. Determination of the Contribution to Surface and Interfacial Tensions of Dispersion Forces in Various Liquids1. *J. Phys. Chem.* **1963**, *67* (12), 2538–2541. https://doi.org/10.1021/j100806a008.

(34) Owens, D. K.; Wendt, R. C. Estimation of the Surface Free Energy of Polymers. *J. Appl. Polym. Sci.* **1969**, *13* (8), 1741–1747. https://doi.org/10.1002/app.1969.070130815.

(35) Jańczuk, B.; Białopiotrowicz, T.; Wójcik, W. The Components of Surface Tension of Liquids and Their Usefulness in Determinations of Surface Free Energy of Solids. *J.*

Colloid Interface Sci. **1989**, *127* (1), 59–66. https://doi.org/https://doi.org/10.1016/0021-9797(89)90007-6.

(36) Tanaka, K.; Fujii, Y.; Atarashi, H.; Akabori, K.; Hino, M.; Nagamura, T. Nonsolvents Cause Swelling at the Interface with Poly(Methyl Methacrylate) Films. *Langmuir* **2008**, *24* (1), 296–301. https://doi.org/10.1021/la702132t.

(37) Yamada, N. L.; Torikai, N.; Mitamura, K.; Sagehashi, H.; Sato, S.; Seto, H.; Sugita, T.; Goko, S.; Furusaka, M.; Oda, T.; Hino, M.; Fujiwara, T.; Takahashi, H.; Takahara, A. Design and Performance of Horizontal-Type Neutron Reflectometer SOFIA at J-PARC/MLF. *Eur. Phys. J. Plus* **2011**, *126* (11), 108. https://doi.org/10.1140/epjp/i2011-11108-7.

(38) Mitamura, K.; Yamada, N. L.; Sagehashi, H.; Torikai, N.; Arita, H.; Terada, M.; Kobayashi, M.; Sato, S.; Seto, H.; Goko, S.; Furusaka, M.; Oda, T.; Hino, M.; Jinnai, H.; Takahara, A. Novel Neutron Reflectometer SOFIA at J-PARC/MLF for in-Situ Soft-Interface Characterization. *Polym. J.* **2013**, *45*, 100–108.

(39) Sowaileh, M. F.; Hazlitt, R. A.; Colby, D. A. Application of the Pentafluorosulfanyl Group as a Bioisosteric Replacement. *ChemMedChem* **2017**, *12* (18), 1481–1490. https://doi.org/https://doi.org/10.1002/cmdc.201700356.

(40) Jagodzinska, M.; Huguenot, F.; Candiani, G.; Zanda, M. Assessing the Bioisosterism of the Trifluoromethyl Group with a Protease Probe. *ChemMedChem* **2009**, *4* (1), 49–51. https://doi.org/10.1002/cmdc.200800321.

(41) Sitzmann, M. E. 1,3,4-Oxadiazoles with SF5-Containing Substituents. *J. Fluor. Chem.* **1995**, *70* (1), 31–38. https://doi.org/https://doi.org/10.1016/0022-1139(94)03095-H.

(42) Welch, J. T.; Lim, D. S. The Synthesis and Biological Activity of Pentafluorosulfanyl Analogs of Fluoxetine, Fenfluramine, and Norfenfluramine. *Bioorg. Med. Chem.* **2007**, *15* (21), 6659–6666. https://doi.org/10.1016/j.bmc.2007.08.012.

(43) Nishino, T.; Urushihara, Y.; Meguro, M.; Nakamae, K. Surface Properties and Structures of Diblock Copolymer and Homopolymer with Perfluoroalkyl Side Chains. *J. Colloid Interface Sci.* **2005**, *283* (2), 533–538. https://doi.org/https://doi.org/10.1016/j.jcis.2004.09.041.

(44) Nishino, T.; Urushihara, Y.; Meguro, M.; Nakamae, K. Surface Properties and Structures of Diblock and Random Copolymers with Perfluoroalkyl Side Chains. *J. Colloid Interface Sci.* **2004**, *279* (2), 364–369. https://doi.org/https://doi.org/10.1016/j.jcis.2004.06.082.

(45) Urushihara, Y.; Nishino, T. Effects of Film-Forming Conditions on Surface Properties and Structures of Diblock Copolymer with Perfluoroalkyl Side Chains. *Langmuir* **2005**, *21* (6), 2614–2618. https://doi.org/10.1021/la047317n.

(46) Ameduri, B.; Bongiovanni, R.; Lombardi, V.; Pollicino, A.; Priola, A.; Recca, A. Effect of the Structural Parameters of a Series of Fluoromonoacrylates on the Surface Properties of Cured Films. *J. Polym. Sci. Part A Polym. Chem.* **2001**, *39* (24), 4227–4235. https://doi.org/https://doi.org/10.1002/pola.10072.

(47) Ameduri, B.; Bongiovanni, R.; Malucelli, G.; Pollicino, A.; Priola, A. New Fluorinated Acrylic Monomers for the Surface Modification of UV-Curable Systems. *J. Polym. Sci. Part A Polym. Chem.* **1999**, *37* (1), 77–87. https://doi.org/https://doi.org/10.1002/(SICI)1099-0518(19990101)37:1<77::AID-POLA9>3.0.CO;2-0.

(48) Honda, K.; Morita, M.; Otsuka, H.; Takahara, A. Molecular Aggregation Structure and Surface Properties of Poly(Fluoroalkyl Acrylate) Thin Films. *Macromolecules* **2005**, *38* (13), 5699–5705. https://doi.org/10.1021/ma050394k.

(49) Atarashi, H.; Hirai, T.; Hori, K.; Hino, M.; Morita, H.; Serizawa, T.; Tanaka, K. Uptake of Water in As-Spun Poly(Methyl Methacrylate) Thin Films. *RSC Adv.* **2013**, *3* (11), 3516–3519. https://doi.org/10.1039/C3RA23066J.

(50) Shimokita, K.; Yamamoto, K.; Miyata, N.; Nakanishi, Y.; Ogawa, H.; Takenaka, M.; Yamada, N. L.; Miyazaki, T. Investigation of Interfacial Water Accumulation between Polypropylene Thin Film and Si Substrate by Neutron Reflectivity. *Langmuir* **2021**, *37* (49), 14550–14557. https://doi.org/10.1021/acs.langmuir.1c02771.

(51) Miyazaki, T.; Miyata, N.; Yoshida, T.; Arima, H.; Tsumura, Y.; Torikai, N.; Aoki, H.; Yamamoto, K.; Kanaya, T.; Kawaguchi, D.; Tanaka, K. Detailed Structural Study on the Poly(Vinyl Alcohol) Adsorption Layers on a Si Substrate with Solvent Vapor-Induced Swelling. *Langmuir* **2020**, *36* (13), 3415–3424. https://doi.org/10.1021/acs.langmuir.9b03964.

(52) Miyazaki, T.; Miyata, N.; Asada, M.; Tsumura, Y.; Torikai, N.; Aoki, H.; Yamamoto, K.; Kanaya, T.; Kawaguchi, D.; Tanaka, K. Elucidation of a Heterogeneous Layered Structure in the Thickness Direction of Poly(Vinyl Alcohol) Films with Solvent Vapor-Induced Swelling. *Langmuir* **2019**, *35* (34), 11099–11107. https://doi.org/10.1021/acs.langmuir.9b01665.

TOC

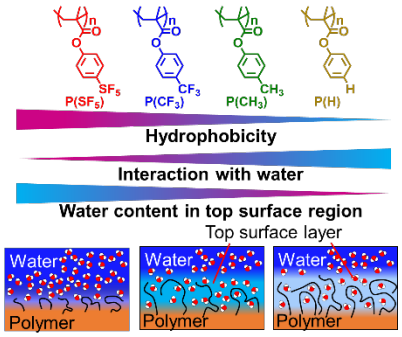
P(SF5)
P(CF3)
P(CH3)
P(H)
Hydrophobicity
Interaction with water
Water content in top surface region
Top surface layer
Water
Polymer
Water
Polymer
Water
Polymer